J Mater Sci (2007) 42:2432–2442
DOI 10.1007/s10853-006-1212-3

Quantitative analysis for kinetics of reactive diffusion in the Fe–Cr system

M. Kajihara · T. Yamashina

Received: 2 November 2005 / Accepted: 23 January 2006 / Published online: 22 December 2006

Abstract In the binary Fe–Cr system, the γ phase with the face-centered cubic structure becomes a stable intermediate phase sandwiched between the Fe-rich α_1 and Cr-rich α_2 phases with the body-centered cubic structure in the temperature range between T = 1,119 and 1,185 K. Within this temperature range, the reactive diffusion between the α_1 and α_2 phases was experimentally observed by Nishizawa and Chiba (Nishizawa and Chiba (1970) J Jap Inst Met 34:629). In their experiment, Fe/Cr diffusion couples were annealed at T = 1,123–1,163 K for up to 600 h. Although the γ phase should be formed due to annealing, it was not recognized in any annealed diffusion couples. The mathematical model reported in a previous study (2004 Acta Mater 52:1193) was used to analyze their experimental results theoretically. In order to provide the boundary conditions for the analysis, the phase diagram in the Fe–Cr system was computed by a CALPHAD technique. The analysis indicates that the γ phase is actually produced at the interface but its thickness is less than 1 μm even after annealing at T = 1,163 K for 600 h. Thus, the γ phase is practically invisible under their experimental conditions. The analysis provides the experimental conditions for the γ phase to grow to observable thicknesses.

M. Kajihara (✉)
Department of Materials Science and Engineering, Tokyo Institute of Technology, Midori-ku, Yokohama 226-8502, Japan
e-mail: kajihara@materia.titech.ac.jp

T. Yamashina
Graduate School, Tokyo Institute of Technology, Midori-ku, Yokohama 226-8502, Japan

Introduction

A reactive diffusion technique may be useful to determine a phase diagram of binary system where many intermediate phases appear as thermodynamically stable phases. In this technique, a diffusion couple composed of two different pure elements is annealed at various temperatures for appropriate times. Due to annealing, the intermediate phases will be produced at the interface in the diffusion couple and then grow with increasing annealing time. When a concentration profile of each element across the interface is measured by electron probe microanalysis (EPMA), the interfacial compositions of the constituent phases will be determined readily. If the local equilibrium is realized at the interface, the determination deduces the boundary compositions of the tie-line between the neighboring phases at the interface. However, all the stable intermediate phases may not be necessarily recognized in the diffusion couple within realistic annealing times. Such cases are actually reported by many investigators for multitudinous binary systems [1–18].

In the unary Fe system at a pressure of 10^5 Pa, the γ phase with the face-centered cubic (f.c.c.) structure is stable at temperatures between T = 1,185 and 1,667 K, and the α phase with the body-centered cubic (b.c.c.) structure becomes stable at $T \leq$ 1,185 K and T = 1,667–1,811 K [19]. The addition of Cr to Fe increases the overall thermodynamic stability of the α phase, but decreases that of the γ phase. As the concentration of Cr increases in the binary Fe–Cr system, the single-phase region of the γ phase at the Fe-rich corner of the

phase diagram becomes smaller, and then finally disappears in the single-phase region of the α phase [19]. As a result, the γ single-phase region is surrounded by the α + γ two-phase region with looped morphology. The α + γ two-phase region with such morphology is usually called the γ loop. Since the γ loop in the Fe–Cr system is convex not only towards the Cr-rich corner but also downwards, a valley appears in the γ loop in the temperature range between T = 1,119 and 1,185 K [19]. This means that a small amount of Cr addition partially increases the thermodynamic stability of the γ phase at lower temperatures. Thus, if a diffusion couple consisting of the Fe-rich α (α_1) phase and the Cr-rich α (α_2) phase is annealed in the temperature range for the valley of the γ loop, the γ phase will be formed at the α_1/α_2 interface after appropriate annealing times due to the reactive diffusion between the α_1 and α_2 phases. Such an experiment was actually carried out by Nishizawa and Chiba [14]. In their experiment, diffusion couples composed of pure Fe and Cr were annealed at T = 1,123–1,163 K for various times up to 600 h. However, the γ phase was not observed in any annealed diffusion couples.

It is pointed out by Castleman and Seigle [4] that the annealing temperature has to be sufficiently high and the annealing time should be long enough to yield the nucleation of all the stable intermediate phases and their growth to observable thicknesses. Kidson and Miller [10] state that the growth rate of the intermediate phase is controlled by the diffusion coefficients and the solubility ranges of the relevant phases in the reactive diffusion. However, any quantitative relationships between the diffusion coefficient and the solubility range were not proposed for the growth rate.

In order to examine such a quantitative relationship, the reactive diffusion was theoretically analyzed for a hypothetical binary system composed of one intermediate phase and two primary solid solution phases in a previous study [20]. The growth of the intermediate phase controlled by the volume diffusion is mathematically modeled in that analysis. The analysis indicates that the most predominant parameters controlling the growth rate are the diffusion coefficient and the solubility range of the growing intermediate phase. In the present study, the experimental results by Nishizawa and Chiba [14] were theoretically analyzed using the mathematical model reported in a previous study [20]. The γ loop in the binary Fe–Cr system was computed by a CALPHAD method [21] in order to provide the boundary conditions for the analysis. The analysis accounts for the experimental results quantitatively.

Summary of observation

The reactive diffusion in the Fe–Cr system was experimentally studied by Nishizawa and Chiba [14] in the temperature range for the valley of the γ loop as already mentioned in Sect. ‘‘Introduction’’. In their experiment, diffusion couples consisting of pure Fe and Cr were annealed at temperatures between T = 1,123 and 1,163 K for various times up to t = 600 h. Here, T and t are the annealing temperature and time, respectively. After annealing, the concentration profile of each element was determined by EPMA along the direction normal to the interface in the Fe/Cr diffusion couple. The results at T = 1,163 K for t = 30, 100, 300 and 600 h are shown as open triangles, rhombuses, squares and circles, respectively, in Fig. 1. In this figure, the ordinate indicates the mol fraction y of Cr, and the abscissa shows the location w measured from the position of the migrating interface. Here, α_1 and α_2 stand for the primary solid solution phases of Fe and Cr, respectively, with the b.c.c. structure, and a vertical dashed-and-dotted line indicates the α_1/α_2 interface. The direction from the α_2 phase side to the α_1 phase side is positive for the location w. As can be seen in Fig. 1, the penetration distances in the α_1 and α_2 phases increase with increasing annealing time. This guarantees that the interdiffusion of Fe and Cr takes place in both phases. Nevertheless, the γ phase cannot be clearly recognized at the interface in the Fe/Cr diffusion couple even at the longest annealing time of t = 600 h.

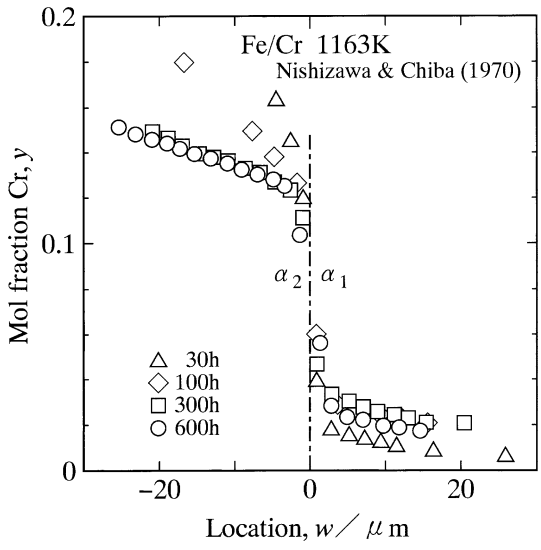

Fig. 1 Concentration profiles of Cr across α_1/α_2 interface in Fe/Cr diffusion couples annealed at 1,163 K for various times between 30 and 600 h by Nishizawa and Chiba [14]

Analysis

The kinetics of the reactive diffusion in a hypothetical binary system consisting of one intermediate phase and two primary solid solution phases was theoretically analyzed in a previous study [20]. In that analysis, the growth rate of the intermediate phase during the reactive diffusion between the primary solid solution phases in a semi-infinite diffusion couple was mathematically expressed using an analytical solution of diffusion equations. Such a mathematical model may be applicable to quantitative analysis of the experimental results by Nishizawa and Chiba [14] on the reactive diffusion in the Fe–Cr system. In the present analysis, the γ loop in the Fe–Cr system has been computed by a CALPHAD method [21]. The computed results have been used as the boundary conditions to calculate the growth rate of the γ phase in a semi-infinite $\alpha_1/\gamma/\alpha_2$ diffusion couple of the Fe–Cr system. Such techniques will be explained briefly.

Computation of γ loop

The Gibbs energy G_m for the α and γ phases in the binary Fe–Cr system can be described as follows:

$$G_m = {}^{o}G_{Fe}(1-y) + {}^{o}G_{Cr}y + RT\{(1-y)\ln(1-y) + y\ln y\} + {}^{E}G_m + {}^{mo}G_m. \quad (1)$$

Here, ${}^{o}G_i$ is the Gibbs energy of pure element i (i = Fe, Cr) for each phase in a hypothetical nonmagnetic state, and R is the gas constant. All of the ${}^{o}G_i$ values are given relative to the molar enthalpy of selected reference states for the elements at T = 298.15 K. This state is denoted by SER (stable element reference) [21]. The excess Gibbs energy ${}^{E}G_m$ may be expressed by the following equation:

$${}^{E}G_m = (1-y)y\{{}^{0}L + {}^{1}L(2y-1)\}. \quad (2)$$

In Eq. 2, the parameters ${}^{0}L$ and ${}^{1}L$ represent thermodynamic interactions between Fe and Cr in each phase. The term ${}^{mo}G_m$ in Eq. 1 indicates the contribution due to magnetic ordering. This contribution can be described using the model suggested by Hillert and Jarl [22] as follows:

$${}^{mo}G_m = RT\ln(\beta+1)f(\tau). \quad (3)$$

Here, β is the average magnetic moment per atom, and τ is defined as

$$\tau \equiv T/T_C. \quad (4)$$

The parameter T_C in Eq. 4 is the Curie or Néel temperature. The function $f(\tau)$ in Eq. 3 is described by

$$f(\tau) = \frac{1}{\tau A}\left\{\tau A - \frac{79}{140p} - \frac{474}{497}\left(\frac{1}{p}-1\right)\left(\frac{\tau^4}{6} + \frac{\tau^{10}}{135} + \frac{\tau^{16}}{600}\right)\right\} \quad (5)$$

and

$$f(\tau) = \frac{-1}{A}\left(\frac{\tau^{-5}}{10} + \frac{\tau^{-15}}{315} + \frac{\tau^{-25}}{1,500}\right) \quad (6)$$

for $\tau < 1$ and $\tau > 1$, respectively. Here, the parameter A is expressed by

$$A = \frac{518}{1,125} + \frac{11,692}{15,975}\left(\frac{1}{p}-1\right). \quad (7)$$

The thermodynamic parameters of the α and γ phases in the Fe–Cr system are evaluated by Andersson and Sundman [23]. The evaluated values are indicated in SI units with R = 8.31451 J/Kmol as follows.

(a) b.c.c.-α phase:

$${}^{o}G^{\alpha}_{Cr} - H^{SER}_{Cr} = -8851.93 + 157.48T - 26.908T\ln T + 1.89435\times10^{-3}T^2 - 1.47721\times10^{-6}T^3 + 1.3925\times10^{5}T^{-1}, 298.15 < T < 2180;$$

$${}^{o}G^{\alpha}_{Cr} - H^{SER}_{Cr} = -34864 + 344.18T - 50T\ln T - 2.88526\times10^{32}T^{-9}, 2180 < T < 6000;$$

$${}^{o}G^{\alpha}_{Fe} - H^{SER}_{Fe} = 1224.83 + 124.134T - 23.5143T\ln T - 4.39752\times10^{-3}T^2 - 5.89269\times10^{-8}T^3 + 7.73585\times10^{4}T^{-1}, 298.15 < T < 1811;$$

$${}^{o}G^{\alpha}_{Fe} - H^{SER}_{Fe} = -25384.451 + 299.31255T - 46T\ln T + 2.2960305\times10^{31}T^{-9}, 1811 < T < 6000;$$

$${}^{0}L^{\alpha} = 20500 - 9.68T,$$

$${}^{1}L^{\alpha} = 0,$$

$$T_C = -311y + 1043(1-y) + y(1-y)\{1650 + 550(2y-1)\},$$

$$\beta = -0.008y + 2.22(1-y) - y(1-y)0.85$$

and

$$p = 0.4.$$

Negative values of T_C and β should be divided by –1.
(b) f.c.c.-γ phase:

$$^{o}G^{\gamma}_{Fe} - {}^{o}G^{\alpha}_{Fe} = -1462.4 + 8.282T - 1.15T\ln T + 6.4 \times 10^{-4}T^2, 298.15 < T < 1811;$$

$$^{o}G^{\gamma}_{Fe} - H^{SER}_{Fe} = -27098.266 + 300.25256T - 46T\ln T + 2.78854 \times 10^{31}T^{-9}, 1811 < T < 6000;$$

$$^{o}G^{\gamma}_{Cr} - {}^{o}G^{\alpha}_{Cr} = 7284 + 0.163T,$$

$$^{0}L^{\gamma} = 10833 - 7.477T$$

and

$$^{1}L^{\gamma} = 1410.$$

It should be noted that the reference state of $^{o}G^{\gamma}_{Fe}$ is selected as H^{SER}_{Fe} at $T > 1{,}181$ K but $^{o}G^{\alpha}_{Fe}$ at $T < 1{,}181$ K in the evaluation.

Analytical solution of diffusion equations

In order to describe mathematically the growth rate of the γ phase during the reactive diffusion in the temperature range for the valley of the γ loop in the Fe–Cr system, we consider a semi-infinite diffusion couple consisting of the α_1 and α_2 phases with initial compositions of $y^{\alpha 10}$ and $y^{\alpha 20}$, respectively. The semi-infinite diffusion couple means that the thickness is semi-infinite for the α_1 and α_2 phases and the α_1/α_2 interface is flat. In such a diffusion couple, the interdiffusion of Fe and Cr takes place unidirectionally along the direction perpendicular to the flat interface. This direction is hereafter designated the diffusional direction. In Fig. 1, the location w on the abscissa is measured from the position of the α_1/α_2 interface at each annealing time along the diffusional direction. In order to describe the migration of the interface, however, it is more suitable to use the distance x measured from the initial position of the α_1/α_2 interface. Furthermore, like the location w in Fig. 1, the direction from the α_2 phase side to the α_1 phase side is considered positive for the distance x.

When the semi-infinite diffusion couple is annealed at a certain temperature T for the valley of the γ loop, a layer of the γ phase will be produced at the interface due to the reactive diffusion between the α_1 and α_2 phases. According to the analysis in a previous study [20], the growth rate of the γ phase during the reactive diffusion is mathematically described with an analytical solution of diffusion equations. In order to deduce such a mathematical description, the following assumptions are adopted in the present study: (A) the local equilibrium is realized at each migrating interface; (B) the migration of the interface is controlled by the volume diffusion in the neighboring phases; (C) the diffusion coefficient for the volume diffusion is independent of the composition in each phase; and (D) the molar volume is independent of the composition and equivalent for all the phases. Although assumption D is not necessary for the deduction, it simplifies the analysis and makes the comparison of the concentration profile with the phase diagram easier. According to assumptions A–C, the positions $z^{\gamma\alpha 1}$ and $z^{\gamma\alpha 2}$ of the migrating γ/α_1 and γ/α_2 interfaces are described as functions of the annealing time t by the equations

$$z^{\gamma\alpha 1} = K^{\gamma\alpha 1}\sqrt{4D^{\gamma}t} = K^{\alpha 1\gamma}\sqrt{4D^{\alpha 1}t} \tag{8a}$$

and

$$z^{\gamma\alpha 2} = K^{\gamma\alpha 2}\sqrt{4D^{\gamma}t} = K^{\alpha 2\gamma}\sqrt{4D^{\alpha 2}t}, \tag{8b}$$

respectively. Here, $D^{\alpha 1}$, $D^{\alpha 2}$ and D^{γ} are the diffusion coefficients in the α_1, α_2 and γ phases, respectively, and $K^{\alpha 1\gamma}$, $K^{\gamma\alpha 1}$, $K^{\alpha 2\gamma}$ and $K^{\gamma\alpha 2}$ are the dimensionless proportionality coefficients. In Eq. 8, $z^{\gamma\alpha 1}$ and $z^{\gamma\alpha 2}$ are measured from the origin of the distance x. As long as the γ phase is thermodynamically stable, it always grows at a finite rate. Thus, $z^{\gamma\alpha 1}$ is greater than $z^{\gamma\alpha 2}$. The thickness l of the γ phase is equal to the difference between $z^{\gamma\alpha 1}$ and $z^{\gamma\alpha 2}$, and hence the following relationship is obtained from Eq. 8:

$$l^2 = (z^{\gamma\alpha 1} - z^{\gamma\alpha 2})^2 = 4D^{\gamma}(K^{\gamma\alpha 1} - K^{\gamma\alpha 2})^2 t = Kt. \tag{9}$$

Equation 9 indicates that the square of the thickness l is proportional to the annealing time t. Such a relationship is usually denoted as the parabolic relationship. The proportionality coefficient K of the parabolic relationship in Eq. 9 is defined as

$$K \equiv 4D^{\gamma}(K^{\gamma\alpha 1} - K^{\gamma\alpha 2})^2. \tag{10}$$

Since $K^{\gamma\alpha 1}$ and $K^{\gamma\alpha 2}$ are dimensionless, K possesses the same dimension as D^{γ} according to Eq. 10. The parameters $K^{\alpha 1\gamma}$, $K^{\gamma\alpha 1}$, $K^{\alpha 2\gamma}$ and $K^{\gamma\alpha 2}$ in Eq. 8 are related with the initial compositions $y^{\alpha 10}$ and $y^{\alpha 20}$ as follows:

$$y^{\gamma\alpha1}-y^{\alpha1\gamma}=\frac{y^{\alpha10}-y^{\alpha1\gamma}}{K^{\alpha1\gamma}\sqrt{\pi}\{1-\mathrm{erf}(K^{\alpha1\gamma})\}}\exp\left\{-\left(K^{\alpha1\gamma}\right)^2\right\}+\frac{y^{\gamma\alpha2}-y^{\gamma\alpha1}}{K^{\gamma\alpha1}\sqrt{\pi}\{\mathrm{erf}(K^{\gamma\alpha1})-\mathrm{erf}(K^{\gamma\alpha2})\}}\exp\left\{-\left(K^{\gamma\alpha1}\right)^2\right\} \tag{11a}$$

and

$$y^{\alpha2\gamma}-y^{\gamma\alpha2}=\frac{y^{\gamma\alpha1}-y^{\gamma\alpha2}}{K^{\gamma\alpha2}\sqrt{\pi}\{\mathrm{erf}(K^{\gamma\alpha1})-\mathrm{erf}(K^{\gamma\alpha2})\}}\exp\left\{-\left(K^{\gamma\alpha2}\right)^2\right\}+\frac{y^{\alpha20}-y^{\alpha2\gamma}}{K^{\alpha2\gamma}\sqrt{\pi}\{1+\mathrm{erf}(K^{\alpha2\gamma})\}}\exp\left\{-\left(K^{\alpha2\gamma}\right)^2\right\}. \tag{11b}$$

Here, $y^{\gamma\alpha1}$ and $y^{\alpha1\gamma}$ are the interfacial compositions of the γ and α_1 phases at the γ/α_1 interface, respectively, and $y^{\gamma\alpha2}$ and $y^{\alpha2\gamma}$ are those of the γ and α_2 phases at the γ/α_2 interface, respectively. According to assumption A, the interfacial compositions coincide with the boundary compositions of the corresponding tie-line at the temperature T. From Eq. 8, the following relationships are readily obtained among the dimensionless proportionality coefficients:

$$K^{\alpha1\gamma}=K^{\gamma\alpha1}\sqrt{D^{\gamma}/D^{\alpha1}} \tag{12a}$$

and

$$K^{\alpha2\gamma}=K^{\gamma\alpha2}\sqrt{D^{\gamma}/D^{\alpha2}}. \tag{12b}$$

Equation 12 shows that only two of $K^{\alpha1\gamma}$, $K^{\gamma\alpha1}$, $K^{\alpha2\gamma}$ and $K^{\gamma\alpha2}$ are independent. In the present analysis, $K^{\gamma\alpha1}$ and $K^{\gamma\alpha2}$ are selected as the independent variables. Such selection is implied by Eq. 10 where K is related with $K^{\gamma\alpha1}$ and $K^{\gamma\alpha2}$. The present selection is quite unprescribed, and thus any combinations of the independent variables are susceptible. Inserting Eq. 12 into Eq. 11, we obtain two independent equations. As a consequence, the two independent variables are conclusively determined from the two independent equations. If the values of $K^{\alpha1\gamma}$, $K^{\gamma\alpha1}$, $K^{\alpha2\gamma}$ and $K^{\gamma\alpha2}$ are determined finally, the composition y is expressed as a function of the distance x and the annealing time t by the following equations in the α_1, γ and α_2 phases:

$$y^{\alpha1}=y^{\alpha10}+\frac{y^{\alpha1\gamma}-y^{\alpha10}}{1-\mathrm{erf}(K^{\alpha1\gamma})}\left\{1-\mathrm{erf}\left(\frac{x}{\sqrt{4D^{\alpha1}t}}\right)\right\},\ x>z^{\gamma\alpha1}; \tag{13a}$$

$$y^{\gamma}=\frac{y^{\gamma\alpha2}}{\mathrm{erf}(K^{\gamma\alpha1})-\mathrm{erf}(K^{\gamma\alpha2})}\left\{\mathrm{erf}(K^{\gamma\alpha1})-\mathrm{erf}\left(\frac{x}{\sqrt{4D^{\gamma}t}}\right)\right\}-\frac{y^{\gamma\alpha1}}{\mathrm{erf}(K^{\gamma\alpha1})-\mathrm{erf}(K^{\gamma\alpha2})}\left\{\mathrm{erf}(K^{\gamma\alpha2})-\mathrm{erf}\left(\frac{x}{\sqrt{4D^{\gamma}t}}\right)\right\},\ z^{\gamma\alpha2}<x<z^{\gamma\alpha1}; \tag{13b}$$

and

$$y^{\alpha2}=y^{\alpha20}+\frac{y^{\alpha2\gamma}-y^{\alpha20}}{1+\mathrm{erf}(K^{\alpha2\gamma})}\left\{1+\mathrm{erf}\left(\frac{x}{\sqrt{4D^{\alpha2}t}}\right)\right\},\ x<z^{\gamma\alpha2}. \tag{13c}$$

Due to assumption D, the mol fraction y of Cr is used to express the composition in Eqs. 11 and 13. Such an expression is practically useful to compare the concentration profile with the phase diagram directly. If assumption D is eliminated, the corresponding equations are obtained by simply replacing y with c in Eqs. 11 and 13 [20]. Here, c is the concentration of Cr measured in mol per unit volume. Between y and c, there exists the relationship $c = y/V_m$ where V_m is the molar volume of the relevant phase.

Results and discussion

Phase diagram

The γ loop in the binary Fe–Cr system was computed by a CALPHAD technique [21] using the thermodynamic parameters evaluated by Andersson and Sundman [23]. The result is shown as solid curves in Fig. 2. In this figure, the ordinate indicates the absolute temperature T, and the abscissa shows the mol fraction y of Cr. According to a recent phase diagram in the Fe–Cr system [19], the valley of the γ loop appears in the temperature range between T = 1,119 and 1,185 K as mentioned earlier. On the other hand, it emerges at T = 1,126–1,185 K in Fig. 2. Hence, the computation slightly underestimates the thermodynamic stability of the γ phase. However, the difference of the temperature range is merely 7 K. Therefore, we may conclude that the valley of the γ loop in the Fe–Cr system is satisfactorily reproduced by the computation. The boundary compositions of the α_1–γ and γ–α_2 tie-lines in Fig. 2 are listed at various temperatures in Table 1.

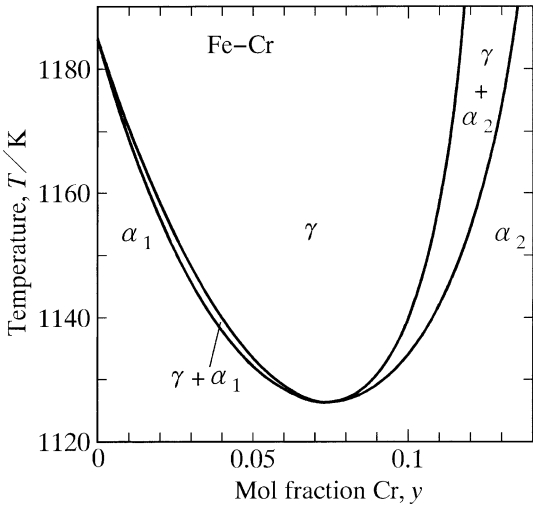

Fig. 2 Phase diagram at Fe-rich corner in the binary Fe–Cr system computed by a CALPHAD technique [21] using the thermodynamic parameters of the α and γ phases [23]

Growth rate of γ phase

According to assumption A, the local equilibrium is realized at each migrating interface during the growth of the γ phase in the $\alpha_1/\gamma/\alpha_2$ diffusion couple. Under such conditions, the interfacial compositions coincide with the boundary compositions of the corresponding tie-line as mentioned in Sect. ''Analytical sloution of diffusion equations''. Therefore, $y^{\alpha 1\gamma}$, $y^{\gamma\alpha 1}$, $y^{\gamma\alpha 2}$ and $y^{\alpha 2\gamma}$ in Table 1 indicate the interfacial compositions. Due to the relationships in Eq. 12, two of $K^{\alpha 1\gamma}$, $K^{\gamma\alpha 1}$, $K^{\alpha 2\gamma}$ and $K^{\gamma\alpha 2}$ are the independent variables in Eq. 11. In the present analysis, $K^{\gamma\alpha 1}$ and $K^{\gamma\alpha 2}$ are arbitrarily chosen as the independent variables as mentioned earlier. Thus, in principle, the two independent variables can be determined from the two independent equations. However, $K^{\gamma\alpha 1}$ and $K^{\gamma\alpha 2}$ are the arguments of the error function and the exponential function in Eq. 11, and hence the determination cannot be carried out in an explicit manner. Consequently, a numerical technique [24] was used to calculate $K^{\gamma\alpha 1}$ and $K^{\gamma\alpha 2}$. The numerical calculation finally provides the value of K through Eq. 10.

Table 1 Boundary compositions of tie-lines for γ loop in the Fe–Cr system computed at various temperatures

T/K	$y^{\alpha 1\gamma}$	$y^{\gamma\alpha 1}$	$y^{\gamma\alpha 2}$	$y^{\alpha 2\gamma}$
1,130	5.52×10^{-2}	5.74×10^{-2}	8.86×10^{-2}	9.22×10^{-2}
1,140	3.71×10^{-2}	4.00×10^{-2}	1.00×10^{-1}	1.08×10^{-1}
1,150	2.56×10^{-2}	2.82×10^{-2}	1.06×10^{-1}	1.17×10^{-1}
1,160	1.67×10^{-2}	1.87×10^{-2}	1.11×10^{-1}	1.23×10^{-1}
1,163	1.43×10^{-2}	1.61×10^{-2}	1.12×10^{-1}	1.25×10^{-1}
1,170	9.23×10^{-3}	1.05×10^{-2}	1.14×10^{-1}	1.28×10^{-1}
1,180	2.81×10^{-3}	3.22×10^{-3}	1.16×10^{-1}	1.32×10^{-1}

The temperature dependence of the diffusion coefficient D is usually described by the equation

$$D = D_0 \exp(-Q/RT). \tag{14}$$

Here, D_0 is the pre-exponential factor, and Q is the activation enthalpy. The following parameters were adopted for the numerical calculation: $D_0 = 1.69 \times 10^{-5}$ m^2/s and $Q = 264$ kJ/mol for the γ phase; and $D_0 = 2.3 \times 10^{-4}$ m^2/s and $Q = 239$ kJ/mol for the α_1 and α_2 phases [25]. The calculation was carried out at $T = 1{,}163$ K under various initial conditions where the initial composition $y^{\alpha 20}$ of the α_2 phase was varied but that $y^{\alpha 10}$ of the α_1 phase was kept constant. At $y^{\alpha 10} = 0$, values of $K = 6.96 \times 10^{-17}$, 9.88×10^{-18}, 2.02×10^{-18} and 4.49×10^{-19} m^2/s are obtained for $y^{\alpha 20} = 0.125$, 0.15, 0.25 and 1, respectively. Using such values of K, the relationship between the thickness l and the annealing time t was evaluated from Eq. 9. The results with $y^{\alpha 20} = 0.125$, 0.15, 0.25 and 1 are shown as solid, dashed, dotted and dashed-and-dotted lines, respectively, in Fig. 3. In this figure, the ordinate and the abscissa indicate the logarithms of l and t, respectively. According to the results in Fig. 3, K monotonically decreases with increasing value of $y^{\alpha 20}$.

The concentration profile of Cr along the diffusional direction in the diffusion couple with $y^{\alpha 10} = 0$ and $y^{\alpha 20} = 1$ was evaluated under the annealing conditions at $T = 1{,}163$ K for $t = 600$ h from Eq. 13. The result is shown as solid curves in Fig. 4. In this figure, the

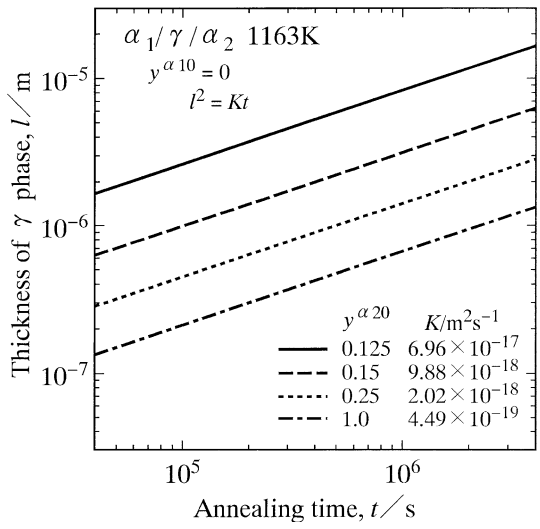

Fig. 3 The thickness l of the γ phase as a function of the annealing time t calculated from Eq. 9 at $T = 1{,}163$ K for $\alpha_1/\gamma/\alpha_2$ diffusion couples with $y^{\alpha 10} = 0$ and $y^{\alpha 20} = 0.125$–1

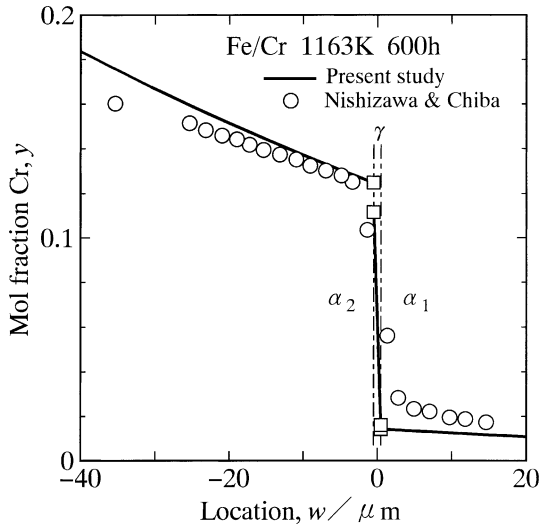

Fig. 4 Concentration profile of Cr along the diffusional direction in $\alpha_1/\gamma/\alpha_2$ diffusion couple with $y^{\alpha 10} = 0$ and $y^{\alpha 20} = 1$ calculated at $T = 1{,}163$ K for $t = 600$ h. The open circles in Fig. 1 are also represented

experimental points for $t = 600$ h in Fig. 1 are also represented as open circles. Here, the ordinate indicates the mol fraction y of Cr, and the abscissa shows the location w. The location w in Fig. 1 is measured from the position of the α_1/α_2 interface in the Fe/Cr diffusion couple. However, the solid curves in Fig. 4 indicate that the γ phase is produced between the α_1 and α_2 phases under the present annealing conditions. Thus, in Fig. 4, the location w is measured from the center of the γ phase in the $\alpha_1/\gamma/\alpha_2$ diffusion couple. If the central position ζ of the γ phase is defined as

$$\zeta \equiv (z^{\gamma\alpha 1} + z^{\gamma\alpha 2})/2, \tag{15}$$

the location w is readily calculated from the distance x by the equation

$$w = x - \zeta. \tag{16}$$

As can be seen in Fig. 4, the open circles lie rather well on the solid curves. According to the dashed-and-dotted line in Fig. 3, $K = 4.49 \times 10^{-19}$ m^2/s for $y^{\alpha 10} = 0$ and $y^{\alpha 20} = 1$. Inserting this value of K and $t = 2.16 \times 10^6$ s (600 h) into Eq. 9, we obtain $l = 0.98$ μm. The experimental points in Figs. 1 and 4 were determined by EPMA. However, the spatial resolution of EPMA is 1–2 μm. Thus, the concentration profile across the γ phase with a thickness of $l = 0.98$ μm cannot be accurately determined by EPMA. As a consequence, the γ phase is not recognized in the Fe/Cr diffusion couples annealed at 1,163 K for various times up to 600 h, even if the nucleation of the γ phase occurs sufficiently fast. At very early stages of the reactive diffusion, however, the concentration gradient is remarkably steep in the γ phase, and hence the corresponding diffusional flux becomes considerable. Under such conditions, the interface reaction may be the bottleneck for the migration of the interface. For the reactive diffusion controlled by the interface reaction, the local equilibrium is not realized at the interface, and thus the interfacial compositions deviate from the compositions of the corresponding tie-line [26]. This type of rate-controlling process is extensively discussed by Nishizawa and Chiba for the reactive diffusion in the Fe–Cr system [14]. On the other hand, the reactive diffusion controlled by the volume diffusion is considered in the present analysis. Thus, at the very early stages, the present analysis may overestimate the growth rate of the γ phase. Nevertheless, the evaluated value of $l = 0.98$ μm is still smaller than the spatial resolution of EPMA.

If the thickness of the γ phase becomes much greater than the spatial resolution of EPMA, we may observe the γ phase. For $y^{\alpha 10} = 0$ and $y^{\alpha 20} = 1$, K is 6.79×10^{-21}, 4.61×10^{-20},1.37×10^{-19}, 3.44×10^{-19}, 8.52×10^{-19} and 2.66×10^{-18} m^2/s at $T = 1{,}130$, 1,140, 1,150, 1,160, 1,170 and 1,180 K, respectively. Using these values of K, the annealing time t_5 for the γ phase to grow to a thickness of $l = 5$ μm was evaluated to be $t_5 = 3.68 \times 10^9$, 5.42×10^8, 1.82×10^8, 7.27×10^7, 2.93×10^7 and 9.40×10^6 s (1.02×10^6, 1.51×10^5, 5.06×10^4, 2.02×10^4, 8.15×10^3 and 2.61×10^3 h) at $T = 1{,}130$, 1,140, 1,150, 1,160, 1,170 and 1,180 K, respectively, from Eq. 9. At such long annealing times, the concentration gradient in the γ phase becomes gentle, and hence the interface reaction is no longer the bottleneck of the reactive diffusion. Consequently, the reactive diffusion will be controlled by the volume diffusion. The evaluation indicates that the growth of the γ phase to observable thicknesses is rather difficult for the Fe/Cr diffusion couple within realistic experimental annealing times at most of the temperatures even for such a rate-controlling process.

In order to find the annealing conditions to permit sufficient growth of the γ phase, the dependence of K on $y^{\alpha 20}$ was calculated at temperatures between $T = 1{,}130$ and 1,180 K. The results for $y^{\alpha 10} = 0$ are shown as solid curves in Fig. 5. In this figure, the ordinate and the abscissa indicate the logarithms of K and $y^{\alpha 20}$, respectively. At each temperature,K monotonically increases with decreasing value of $y^{\alpha 20}$, and then reaches to the maximum at $y^{\alpha 20} = y^{\alpha 2\gamma}$. Furthermore, the higher the temperature T is, the larger the value of K becomes. If $l > 5$μm, the γ phase may be clearly detected by EPMA. In order to realize $l > 5$μm at $t = 2.16 \times 10^6$ s (600 h), K should be greater than

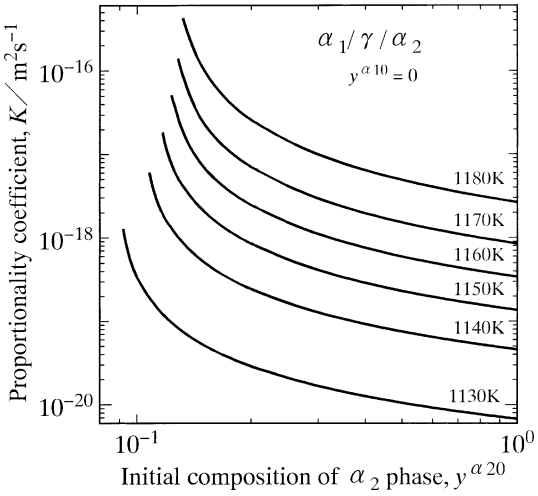

Fig. 5 Dependence of the proportionality coefficient K on the initial composition $y^{\alpha 20}$ of the α_2 phase calculated for $\alpha_1/\gamma/\alpha_2$ diffusion couple with $y^{\alpha 10} = 0$ at temperatures between T = 1,130 and 1,180 K

1.16×10^{-17} m^2/s according to Eq. 9. However, such conditions are actualized only in an area with large values of T and small values of $y^{\alpha 20}$ in Fig. 5.

The calculations in Fig. 5 are represented in a different manner in Fig. 6. In this figure, the ordinate indicates the logarithm of K, and the abscissa shows the reciprocal of T. Solid curves indicate the calculations for $y^{\alpha 20} = 0.15$, 0.25 and 1. As can be seen, K monotonically decreases with decreasing temperature T. If the temperature dependence of K is expressed by a formula similar to Eq. 14, the solid curves in Fig. 6 should be straight. Such a diagram with straight lines is usually called the Arrhenius-type diagram. However, in Fig. 6, the slope of each solid curve changes

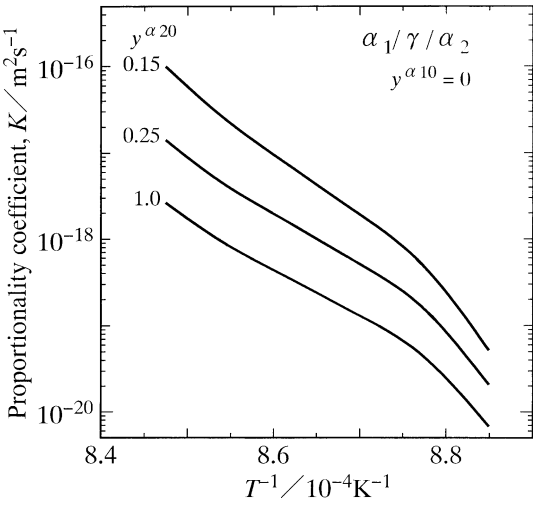

Fig. 6 The results in Fig. 5 represented as K versus T^{-1}

depending on the temperature in a rather complicated manner. Thus, the Arrhenius-type diagram cannot be applicable to the temperature dependence of K. According to Eq. 10, K is a function of D^{γ}, $K^{\gamma\alpha 1}$ and $K^{\gamma\alpha 2}$. Furthermore, $K^{\gamma\alpha 1}$ and $K^{\gamma\alpha 2}$ are functions of $y^{\alpha 10}$, $y^{\alpha 1\gamma}$, $y^{\gamma\alpha 1}$, $y^{\gamma\alpha 2}$, $y^{\alpha 2\gamma}$, $y^{\alpha 20}$, $D^{\alpha 1}$, D^{γ} and $D^{\alpha 2}$ through Eqs. 11 and 12. Hence, K becomes a function of these nine parameters. Although $y^{\alpha 10}$ and $y^{\alpha 20}$ remain constant for each solid curve in Fig. 6, K is still a function of the other seven parameters. The phase diagram in Fig. 2 shows extraordinary temperature dependencies of the boundary compositions $y^{\alpha 1\gamma}$, $y^{\gamma\alpha 1}$, $y^{\gamma\alpha 2}$ and $y^{\alpha 2\gamma}$. On the other hand, the temperature dependence is simply expressed by Eq. 14 for $D^{\alpha 1}$, D^{γ} and $D^{\alpha 2}$. Hence, the temperature dependencies of $y^{\alpha 1\gamma}$, $y^{\gamma\alpha 1}$, $y^{\gamma\alpha 2}$ and $y^{\alpha 2\gamma}$ predominantly affect the curvature for the solid curves in Fig. 6.

Migration rate of γ phase

According to the definition of Eq. 15, the parameter ζ indicates the central position of the γ phase. The central position ζ may be conveniently used to represent the overall migration of the γ phase in the $\alpha_1/\gamma/\alpha_2$ diffusion couple. Inserting Eq. 8 into Eq. 15, we obtain the following equation:

$$\zeta = \left(K^{\gamma\alpha 1} + K^{\gamma\alpha 2}\right)\sqrt{D^{\gamma}t} = k\sqrt{t}. \tag{17}$$

Here, k is the proportionality coefficient defined as follows:

$$k \equiv \left(K^{\gamma\alpha 1} + K^{\gamma\alpha 2}\right)\sqrt{D^{\gamma}}. \tag{18}$$

Equation 17 shows that the central position ζ is proportional to the square root of the annealing time t. It is another formula of the parabolic relationship. However, unlike K in Eq. 9, k in Eq. 17 possesses a dimension of m/s$^{1/2}$. The dependence of k on $y^{\alpha 20}$ was calculated at various temperatures of T = 1,130–1,180 K from Eqs. 11, 12 and 18. The results for $y^{\alpha 10} = 0$ are shown as thin solid curves in Fig. 7. In this figure, the ordinate indicates k, and the abscissa shows the logarithm of $y^{\alpha 20}$. At each temperature, k is negative at $y^{\alpha 20} = y^{\alpha 2\gamma}$, and monotonically increases from negative values to positive values with increasing value of $y^{\alpha 20}$. As mentioned earlier, the γ phase necessarily grows at a certain rate as long as it is thermodynamically stable [20]. Consequently, $z^{\gamma\alpha 1}$ is always greater than $z^{\gamma\alpha 2}$, and hence the term $K^{\gamma\alpha 1}$–$K^{\gamma\alpha 2}$ in Eq. 9 becomes positive. On the contrary, $K^{\gamma\alpha 1}$ and $K^{\gamma\alpha 2}$ themselves take positive or negative values depending on the initial and boundary conditions.

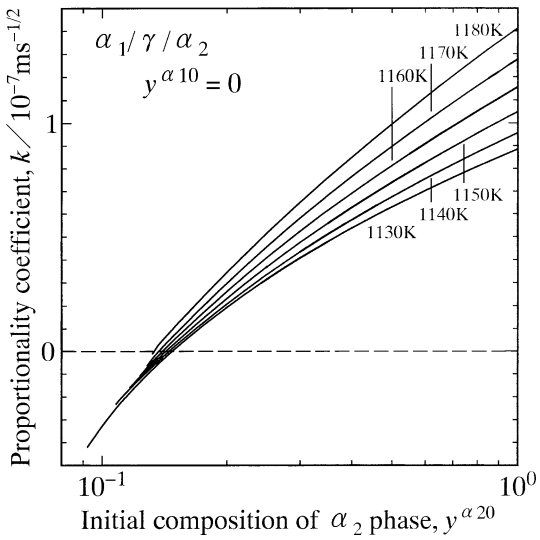

Fig. 7 Dependence of the proportionality coefficient k on the initial composition $y^{\alpha 20}$ of the α_2 phase calculated for $\alpha_1/\gamma/\alpha_2$ diffusion couple with $y^{\alpha 10} = 0$ at temperatures between T = 1,130 and 1,180 K

Therefore, k becomes positive or negative through Eq. 18. The γ phase overall migrates from the α_2 phase side to the α_1 phase side for $k > 0$ but towards the opposite direction for $k < 0$. For $y^{\alpha 10} = 0$ and $y^{\alpha 20} = 1$, the calculation yields $k = 1.19 \times 10^{-7}$ m/s$^{1/2}$ at T = 1,163 K. Using this value of k, the central position ζ was evaluated as a function of the annealing time t from Eq. 17. The result is shown as a solid line in Fig. 8. In this figure, the ordinate and the abscissa indicate the logarithms of ζ and t, respectively. Since k is positive for the solid line in Fig. 8, the γ phase overall migrates from the α_2 phase side to the α_1 phase side under the present initial and boundary conditions.

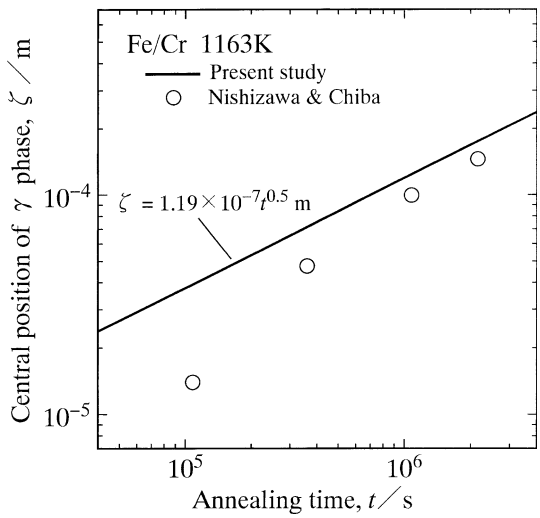

Fig. 8 The central position ζ of the γ phase as a function of the annealing time t calculated at T = 1,163 K for $\alpha_1/\gamma/\alpha_2$ diffusion couple with $y^{\alpha 10} = 0$ and $y^{\alpha 20} = 1$. The experimental results by Nishizawa and Chiba [14] are also shown as open circles

In the experiment by Nishizawa and Chiba [14], the γ phase was invisible in the Fe/Cr diffusion couple even at the longest annealing time. Thus, they observed the position of the α_1/α_2 interface as a function of the annealing time at 1,163 K. However, the present analysis indicates that the γ phase with a thickness of about 1 μm is formed between the α_1 and α_2 phases due to annealing for t = 600 h at T = 1,163 K. Hence, the position of the α_1/α_2 interface practically corresponds to the central position ζ. The values of ζ determined by Nishizawa and Chiba [14] are indicated as open circles in Fig. 8. As can be seen, ζ is positive, and thus the α_1/α_2 interface migrates from the α_2 phase side to the α_1 phase side in their experiment. However, the open circles are located below the solid line. Furthermore, the parabolic relationship does not seem applicable to the open circles.

In the present analysis, the temperature dependence of the diffusion coefficient D is expressed by Eq. 14 using $D_0 = 2.3 \times 10^{-4}$ m^2/s and Q = 239 kJ/mol for the α phase and $D_0 = 1.69 \times 10^{-5}$ m^2/s and Q = 264 kJ/mol for the γ phase. Such parameters of the α and γ phases are the values reported for the self-diffusion coefficient of ^{51}Cr in b.c.c.-Fe $D_{\mathrm{Cr}}^{\alpha-\mathrm{Fe}}$ at T = 1,048–1,971 K and that in f.c.c.-Fe $D_{\mathrm{Cr}}^{\gamma-\mathrm{Fe}}$ at T = 1,173–1,618 K, respectively [25]. Using these parameters, $D^{\alpha} = 6.71 \times 10^{-15}$ m^2/s and $D^{\gamma} = 3.90 \times 10^{-17}$ m^2/s are evaluated at T = 1,185 K from Eq. 14. On the other hand, the molar volumes of the α and γ phases at T = 1,185 K are estimated to be $V_{\mathrm{m}}^{\alpha} = 7.37 \times 10^{-6}$ m^3/mol and $V_{\mathrm{m}}^{\gamma} = 7.30 \times 10^{-6}$ m^3/mol from the lattice parameters a = 0.2904 and 0.3647 nm for b.c.c.-Fe and f.c.c.-Fe, respectively [27]. Thus, we obtain ratios of $D^{\alpha}/D^{\gamma} = 172$ and $V_{\mathrm{m}}^{\alpha}/V_{\mathrm{m}}^{\gamma} = 1.01$. Although these ratios will slightly vary depending on the temperature and the compositions of the α and γ phases, the difference between V_{m}^{α} and V_{m}^{γ} is negligible compared with that between D^{α} and D^{γ}. Consequently, we may conclude that assumption D hardly violates the validity of the present analysis. On the contrary, D^{α} and D^{γ} are treated as independent of the compositions of the α and γ phases, respectively, according to assumption C. However, the self-diffusion coefficient of ^{55}Fe in b.c.c.-Cr $D_{\mathrm{Fe}}^{\mathrm{Cr}}$ is smaller than $D_{\mathrm{Cr}}^{\alpha-\mathrm{Fe}}$ [25]. This implies that D^{α} and D^{γ} vary depending on the compositions of the α and γ phases, respectively. If there exist composition dependencies in D^{α} and D^{γ}, Eqs. 8–13 become invalid. This may be the reason why the parabolic relationship does not hold good for the open circles in Fig. 8.

According to the phase diagram in Fig. 2, the solubilities of Cr in the α_1 and γ phases are smaller than $y = 0.08$ and 0.12, respectively, in the temperature range for the valley of the γ loop. At such small concentrations of Cr, $D^{\alpha 1}$ and D^{γ} can be close to $D_{\mathrm{Cr}}^{\alpha-\mathrm{Fe}}$ and $D_{\mathrm{Cr}}^{\gamma-\mathrm{Fe}}$, respectively. On the other hand, the solubility range of the α_2 phase is much greater than those of the α_1 and γ phases. Hence, there should exist composition dependence in $D^{\alpha 2}$. At short annealing times, the penetration distance due to the interdiffusion is very small in each phase of the $\alpha_1/\gamma/\alpha_2$ diffusion couple. In such a case, the value of $D^{\alpha 2}$ averaged over the penetration distance in the α_2 phase may be smaller than $D_{\mathrm{Cr}}^{\alpha-\mathrm{Fe}}$ but greater than $D_{\mathrm{Fe}}^{\mathrm{Cr}}$. If $D^{\alpha 2}$ takes such an average value smaller than $D^{\alpha 1}$, the overall migration of the γ phase towards the α_1 phase side will decelerate devolving on the diffusional flux balance between the α_1 and α_2 phases [20]. Therefore, at short annealing times, the open circles are located remarkably below the solid line in Fig. 8.

At long annealing times, however, the penetration distance becomes sufficiently large. Under such conditions, the diffusional fluxes in the neighboring phases at each interface are predominantly determined by the diffusion coefficients at the compositions in the vicinity of the interface. As shown in Fig. 2, the composition $y^{\alpha 2\gamma}$ of the α_2 phase at the γ/α_2 interface is smaller than 0.14 in the temperature range for the valley of the γ loop. For such small values of $y^{\alpha 2\gamma}$, $D^{\alpha 2}$ may be rather close to $D^{\alpha 1}$, and almost independent of the composition. Hence, assumption C will become valid. Consequently, at long annealing times, the open circles approach the solid line in Fig. 8. The annealing time t_5 for the γ phase to grow to a thickness of $l = 5$ μm was evaluated at various temperatures in Sect. ''Growth rate of γ phase''. The evaluation results in $t_5 = 2.61 \times 10^3$–1.02×10^6 h at $T = 1{,}180$–$1{,}130$ K, respectively, as mentioned earlier. These values of t_5 are much greater than the longest annealing time of $t = 600$ h in the experiment by Nishizawa and Chiba [14]. At such large values of t_5, the open circles are expected to lie well on the solid line in Fig. 8. Thus, it is concluded that the present analysis yields reliable estimation for the annealing conditions to allow sufficient growth of the γ phase in the Fe/Cr diffusion couple.

Conclusions

The reactive diffusion between the Fe-rich α_1 phase and the Cr-rich α_2 phase in the binary Fe–Cr system was experimentally observed by Nishizawa and Chiba [14] within the temperature range for the valley of γ loop. In their experiment, the diffusion couples consisting of pure Fe and Cr were annealed at temperatures of $T = 1{,}123$ and 1,163 K for various times up to $t = 600$ h. Since the γ phase is the stable intermediate phase at the experimental annealing temperatures [19], it should be formed at the α_1/α_2 interface during annealing. However, the γ phase was not clearly recognized in any annealed diffusion couples. In the present study, such experimental results were theoretically analyzed using the mathematical model reported in a previous study [20]. For the analysis, the following assumptions were adopted: (A) the local equilibrium is realized at the interface; (B) the migration of the interface is controlled by the volume diffusion; (C) the diffusion coefficient is independent of the composition; and (D) the molar volume is independent of the composition and equivalent for all the phases. In order to provide the boundary conditions for the mathematical model, the γ loop in the Fe–Cr system was computed by a CALPHAD technique [19]. According to the analysis, the γ phase is formed at the α_1/α_2 interface under the experimental annealing conditions. However, the thickness of the γ phase is less than 1 μm even after annealing at $T = 1{,}163$ K for $t = 600$ h. The analysis yields the experimental conditions for the γ phase to grow to observable thicknesses.

Acknowledgements The authors are grateful to Professor K. Ishida at Tohoku University, Japan for stimulating discussions. The present study was supported by a Grant-in-Aid for Scientific Research from the Ministry of Education, Culture, Sports, Science and Technology of Japan.

References

1. Lustman B, Mehl RF (1942) Trans Met Soc AIME 147:369
2. Horstmann D (1953) Stahl Eisen 73:659
3. Storchheim S, Zambrow JL, Hausner HH (1954) Trans Met Soc AIME 200:269
4. Castleman LS, Seigle LL (1957) Trans Met Soc AIME 209:1173
5. Castleman LS, Seigle LL (1958) Trans Met Soc AIME 212:589
6. Peterson NL, Ogilvie RE (1960) Trans Met Soc AIME 218:439
7. Adda Y, Beyeler M, Kirianenko A, Mauruce MF (1961) Mem Sci Rev Met 58:716
8. Birks LS, Seebold RE (1961) J Nucl Mater 3:249
9. Seebold RE, Birks LS (1961) J Nucl Mater 3:260
10. Kidson GV, Miller GD (1964) J Nucl Mater 12:61
11. Sweeney WE, Jr., Batt AP (1964) J Nucl Mater 13:87
12. Shibata K, Morozumi S, Koda S (1966) J Japan Inst Met 30:382
13. Hirano K, Ipposhi Y (1968) J Japan Inst Met 32:815
14. Nishizawa T, Chiba A (1970) J Japan Inst Met 34:629
15. Kajihara M, Yamada T, Miura K, Kurokawa N, Sakamoto K (2003) Netsushori 43:297

16. Yamada T, Miura K, Kajihara M, Kurokawa N, Sakamoto K (2004) J Mater Sci 39:2327
17. Yamada T, Miura K, Kajihara M, Kurokawa N, Sakamoto K (2005) Mater Sci Eng A 390:118
18. Mita M, Kajihara M, Kurokawa N, Sakamoto K (2005) Mater Sci Eng A, 403:269
19. Massalski TB, Okamoto H, Subramanian PR, Kacprzak L (1990) In: Binary Alloy Phase Diagrams, vol 2. ASM International, Materials Park, Ohio, p 1273
20. Kajihara M (2004) Acta Mater 53:1193
21. Hillert M (1986). In: Bennett LH (eds), Computer modeling of phase diagrams. TMS-AIME, Warrendale Pennsylvania, p 1
22. Hillert M, Jarl M (1978) Calphad 2:227
23. Andersson J-O, Sundman B (1987) Calphad 11:83
24. Dahlquist G, Björck A (1974) Numerical methods. Prentice-Hall Inc, Englewood Cliffs New Jersey, p 248
25. Metals Data Book (1993) edited by Japan Inst Met. Maruzen, Tokyo, p 21
26. Sutton AP, Balluffi RW (1995) Interfaces in crystalline materials. Oxford Science Publications, Clarendon Press, Oxford, p 603
27. Metals Hand Book (2000) edited by Japan Inst Met. Maruzen, Tokyo, p 473